Nonlinear System Identification of Reinforced Concrete Steel Structure: Using Pseudodynamic Testing Data

Olga V. Pavlenko[1] and Chin-Hsiung Loh, M.ASCE[2]

Abstract: The research results are presented of the joint project of the National Center for Research on Earthquake Engineering (Taiwan) and Stanford University on the pseudodynamic testing of a three-story full-scale reinforced concrete steel moment frame. Nonlinear stress–strain relations, corresponding to oscillations in the frame, were estimated for successive time intervals from a pseudodynamic test of strong ground motion excitation. Numerical models of the behavior of the frame under the pseudodynamic loading of four levels of input ground motion were constructed and used for estimating changes in the shear moduli in the frame during its loading and for the nonlinear identification of the frame behavior. The contents of linear and nonlinear quadratic and cubic components in the response of the frame were estimated. It was found that the frame possesses mostly odd-order nonlinearities, such as the third, fifth, seventh, etc. order nonlinearities, whereas, even-order nonlinearities, such as, quadratic, the fourth, sixth, eighth, etc. order nonlinearities, are weak. Temporal changes in the behavior of the frame were observed during the test, indicating a substantial decrease in the elastic shear moduli, increase in the absorption of seismic waves and in the contents of the nonlinear part in the response of the frame.

DOI: 10.1061/(ASCE)0733-9399(2004)130:7(836)

CE Database subject headings: Pseudodynamic method; Data analysis; Numerical models; Full-scale tests; Building frames; Ground motion.

Introduction

A joint project of the National Center for Research on Earthquake Engineering (NCREE) in Taiwan and Stanford Univ. on testing of a three-story full-scale reinforced concrete steel (RCS) composite moment frame was carried out in October 2002. The test specimen, 12 m tall and 21 m long, was a three-story, three-bay ''RCS'' moment frame, consisting of reinforced concrete columns and composite steel beams, as shown in Fig. 1. The frame was among the largest specimens of its type ever tested with pseudodynamic loading. This three-story prototype structure was designed for areas of high seismicity following provisions for composite structures of the International Building Code 2000. During the test, the frame was loaded pseudodynamically by using input ground motions from the 1999 Chi-Chi and 1989 Loma Prieta earthquakes. The tests were conducted according to the following schedule:

1. October 11, 9:00 a.m.—the imposed motion was the 1999 Chi-Chi Earthquake, station TCU082, EW component, scaled to represent the seismic intensity level of the 50% probability of exceedance in 50 years (PGA$=0.276g$).
2. October 14, 9:00 a.m.—the imposed motion was the 1989 Loma Prieta Earthquake, station LP89g04, NS component, scaled to represent the seismic intensity level of the 10% probability of exceedance in 50 years (PGA$=0.426g$).
3. October 15, 9:00 a.m.—the imposed motion was the 1999 Chi-Chi Earthquake, station TCU082, EW component, scaled to represent the seismic intensity level of the 2% probability of exceedance in 50 years (PGA$=0.622g$).
4. October 16, 9:00 a.m.—the imposed motion was the 1989 Loma Prieta Earthquake, station LP89g04, NS component, scaled to represent the seismic intensity level of the 10% probability of exceedance in 50 years (PGA$=0.426g$).

The input acceleration waveform is shown in Fig. 2. Displacements and force (collected from the load cell of actuator) were recorded at the floor level of the three stories of the frame. Fig. 3 shows the recorded displacements at each floor level from the four different tests.

As a whole, the test had the following primary objectives: to provide data for evaluation and validation the design provisions for composite moment frames (strong-column weak-beam criterion, composite action of concrete slab and steel beams, integrity of the precast column and composite beam–column connections, and overall frame response); to provide information for validating simulation models and computer codes for nonlinear simulation and performance assessment; and to support the use of innovative composite moment frames as alternatives to conventional steel and concrete systems for regions of high seismicity. Based on the assumption of time-varying system, the modal natural frequencies were estimated (Loh et al. 2003). Because of severe intensity of excitation on the frame structure it is believed that nonlinear responses of the frame structure can be observed from the experimental data. To observe the dynamic characteristics of the structure nonlinear system identification must be used.

The successful development of identification procedures for a nonlinear system depends upon the model which is used to represent the system under investigation. Experimental analysis of nonlinear systems may be accomplished by using time domain

[1]Visiting Research Fellow, National Center for Research on Earthquake Engineering, Taipei 106-17, Taiwan, Republic of China.

[2]Professor, Dept. of Civil Engineering, National Taiwan Univ., Taipei 106-17, Taiwan, Republic of China. E-mail: lohc0220@ccms.ntu.edu.tw

Note. Associate Editor: Roger G. Ghanem. Discussion open until December 1, 2004. Separate discussions must be submitted for individual papers. To extend the closing date by one month, a written request must be filed with the ASCE Managing Editor. The manuscript for this paper was submitted for review and possible publication on August 4, 2003; approved on December 23, 2003. This paper is part of the ***Journal of Engineering Mechanics***, Vol. 130, No. 7, July 1, 2004. ©ASCE, ISSN 0733-9399/2004/7-836–847/$18.00.

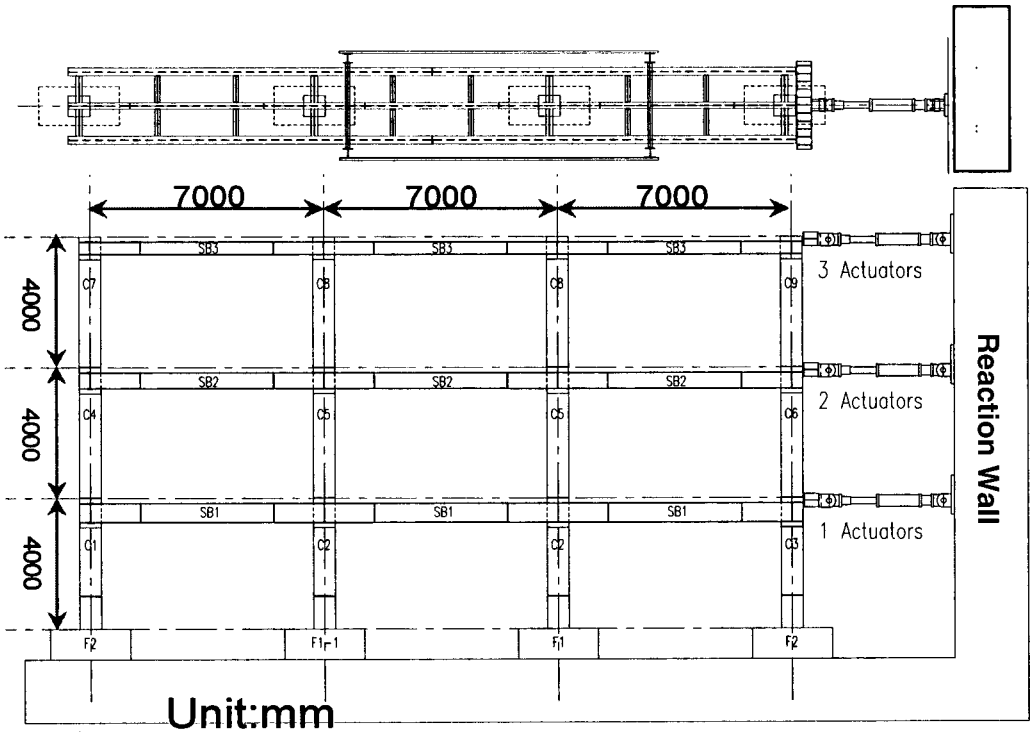

Fig. 1. Dimensions of three-story reinforced concrete steel frame from side view and top view

models. Efforts have been devoted to establish the models of a nonlinear hysteretic system and various techniques are developed by many researchers to identify the model parameters. Experimental analysis of nonlinear systems may be accomplished by using time domain models. Traditionally the functional series descriptions of Volterra and Wiener have been used (Schetzen 1980). Unfortunately, functional series models require excessive kernel values. However, by expanding the system output in terms of past input and output using a nonlinear autoregressive moving average model with exogenous inputs model, a very concise representation for a wide class of nonlinear systems can be obtained (Korenberg et al. 1987; Hunter et al. 1990; Loh and Duh 1996).

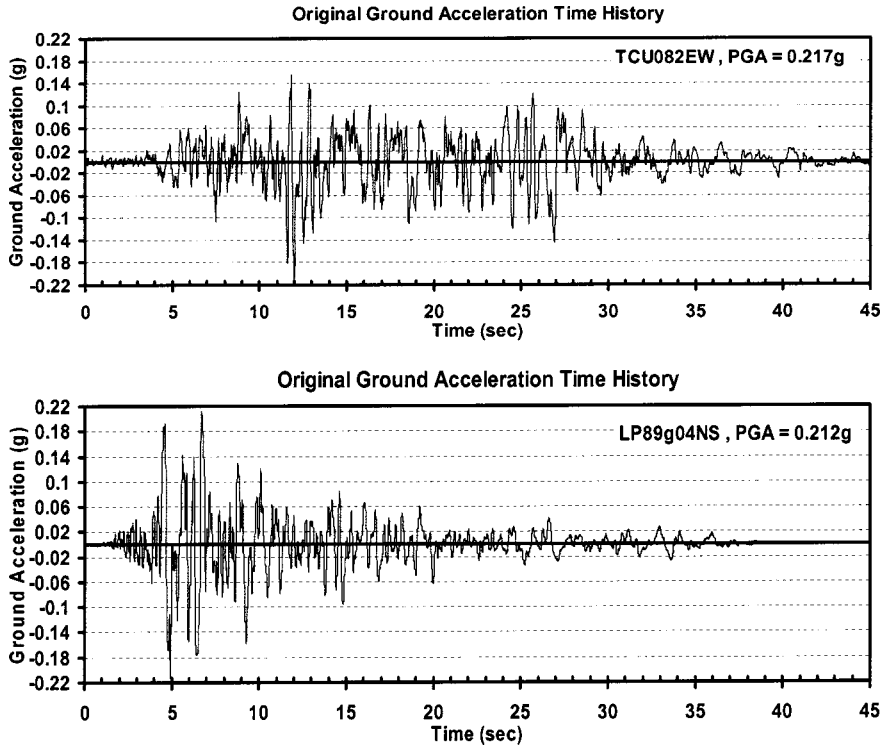

Fig. 2. Two original ground acceleration time histories from Chi-Chi earthquake and Loma Prieta earthquake for input acceleration in pseudodynamic test

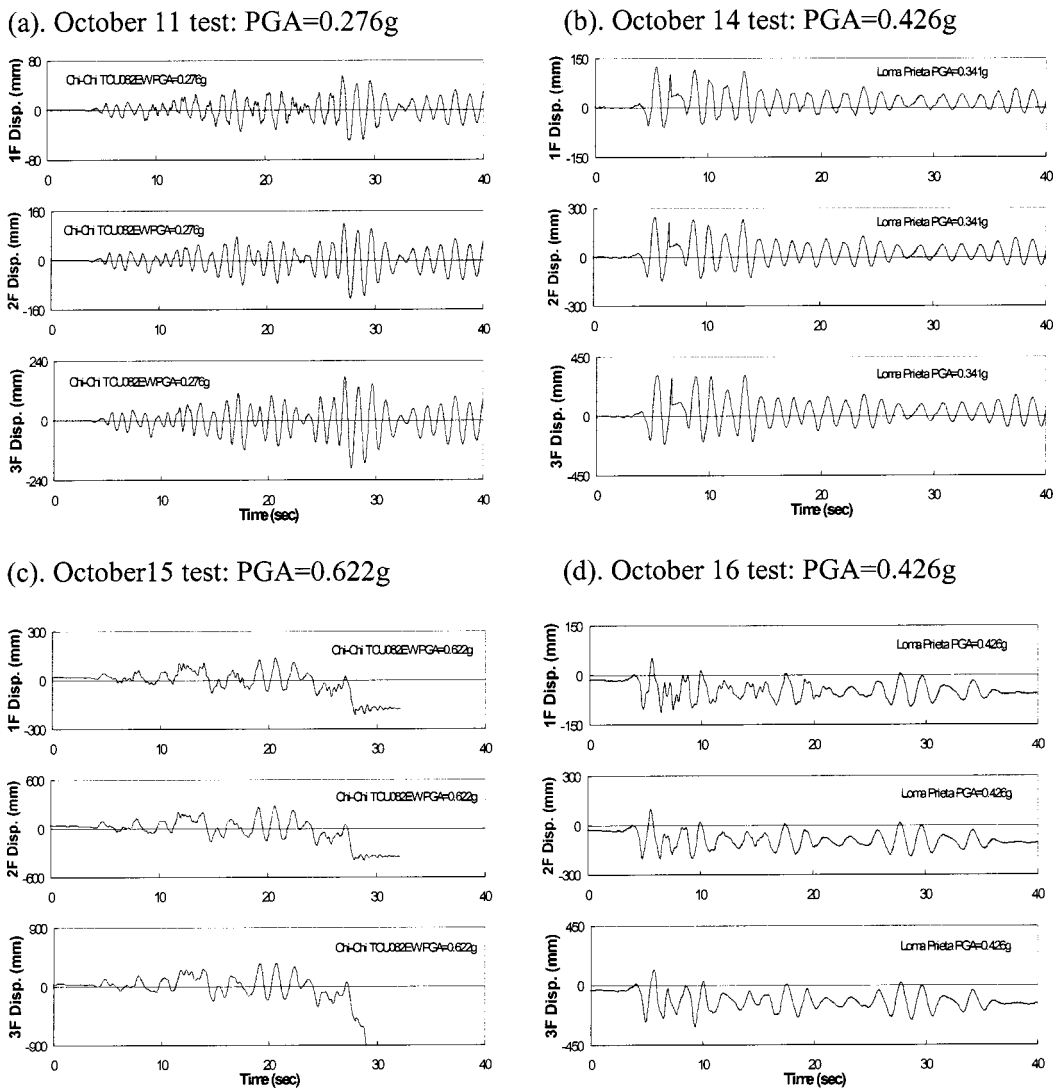

Fig. 3. Recorded displacement at each floor level from four different tests

Based on the assumption of a time-varying system the response of the test data was analyzed and the time-varying modal frequency was investigated (Loh et al. 2003).

In this study the results of the test were used for validating the possibility of applying the method for estimation of nonlinear stress–strain relations (Pavlenko and Irikura 2003), for studying the response of the frame. Another goal of the present work was the nonlinear identification of the behavior of the frame, and estimation of the contents of linear and nonlinear components in the response of the frame in conditions of the applied dynamic loading.

Shear Stress–Strain Response Analysis

A simple identification procedure, which was proposed and used to study the downhole earthquake response, was adapted in this study to identify the nonlinear response of the frame structure. Using the shear beam model to describe the lateral response, shear stresses at levels z_i and $(z_{i-1}+z_i)/2$ may be evaluated as follows:

$$\tau_i(t)=\tau_{i-1}(t)+\rho_{i-1}\frac{\ddot{u}_{i-1}+\ddot{u}_i}{2}\Delta z_{i-1} \quad i=2,3,\ldots \tag{1a}$$

$$\tau_{i-1/2}(t)=\tau_{i-1}(t)+\rho_{i-1}\frac{3\ddot{u}_{i-1}+\ddot{u}_i}{8}\Delta z_{i-1} \quad i=2,3,\ldots \tag{1b}$$

in which subscripts i and $i-1/2$ refer to levels z_i (of the ith accelerometer) and $(z_{i-1}+z_i)/2$ [halfway between accelerometers I and $(i-1)$] respectively, $\tau_i(t)=\tau(z_i;t)$, $\tau_1=\tau(0;t)=0$ at the stress-free surface; ρ_{i-1}=mass density of the z_{i-1} to z_i layer; $\ddot{u}_i=\ddot{u}(z_i,t)$=absolute acceleration at level z_i; and Δz_i=spacing interval between accelerometers. The corresponding second-order accurate shear strains may be expressed as

$$\gamma_i(t)=\frac{1}{\Delta z_{i-1}+\Delta z_i}\left[(u_{i+1}-u_i)\frac{\Delta z_{i-1}}{\Delta z_i}+(u-u_{i-1})\frac{\Delta z_i}{\Delta z_{i-1}}\right]$$

$$\text{for } i=2,3,\ldots \tag{2a}$$

$$\gamma_{i-1/2}(t)=\frac{u_i-u_{i-1}}{\Delta z_{i-1}} \quad \text{for } i=2,3,\ldots \tag{2b}$$

in which $u_i=u(z_i,t)$=absolute displacement [evaluated through double integration of the recorded acceleration history $\ddot{u}(z_i,t)$]. In this study, $u_i\,(i=1-3)$ and $\ddot{u}_i\,(i=1-3)$ represent the dis-

placement and force recorded from the actuator attached at each floor of the RCS frame. Simultaneous recording of τ and γ gives us a representation of the behavior of the frame.

Methods of Data Processing

To carry out the nonlinear identification of the frame responses, knowledge of the nonlinear stress–strain relations in the frame, corresponding to the applied loading in various time intervals, is necessary. To estimate stresses and strains, occurring in the frame during the process of its loading, the modified method of the estimation of stress–strain relations in successive time intervals was used. The procedure of estimation of stress–strain relations in soils in strong ground motion is described in detail in the paper by Pavlenko and Irikura (2003). To estimate stresses and strains in this system studied (frame structure), in this study we calculate acceleration time histories at points of locations of the recording devices, at the three floors of the frame. For calculations, sets of parametric stress–strain relations of a certain type were generated (250 stress–strain relations), and item-by-item examination was applied to identify the relations showing the best-fit approximation between the observed and simulated records.

For calculations, we used the modified algorithm by Joyner and Chen (1975). To describe the behavior of the frame under the applied dynamic loading, we selected stress–strain relations of the most common type, similar to those used to describe the behavior of water-saturated soils. This choice was based on the records obtained in the test. In the domain of small strains, these stress–strain curves are close to linear ones, then they decline to the strain axis with increasing strain (i.e., stress and stiffness degradation) and, if strains increase more, the curves decline to the stress axis. This type of stress–strain relationship, if defined parametrically, represents the most common case because it can account for all the features in the behavior of a frame in conditions of loading. The records obtained in the test indicate that this type of stress–strain relation is also observed in the behavior of the frame under dynamic loading.

To account for temporal changes in the behavior of the frame, the records were divided by time intervals of 2.8 s duration, and successive time intervals were analyzed. The value of 2.8 s was selected to satisfy, on one hand, the condition of the invariability of stress–strain relations within each time interval (the intervals should be short enough); on the other hand, the condition of a rather long duration of analyzed intervals of records for obtaining reliable estimates.

Results and Discussion

The results of the simulations are given in Figs. 4(a–d). These figures show the observed and simulated accelerograms for the four stages of the test. The ''observed'' accelerations were calculated based on the recorded force at the three floors of the frame. A fairly good agreement between the observed and simulated records testifies to the validity of the representation obtained.

Fig. 5(a) represents the stress–strain relations obtained for the four stages of the test (denoted as 1, 2, 3, and 4), which characterize the behavior of the frame under the applied dynamic loading in successive time intervals. According to our estimates, strain values did not exceed the limits of about ± 0.04, and stresses lay within the interval of about ± 8 kPa [Fig. 5(a)]. The stress–strain relations obtained represent the model of the behavior of the frame under the applied dynamic loading. A rather good agreement between the simulated and observed accelerograms indicates that the model is a rather good approximation to the real behavior of the frame. The stress–strain relations obtained show temporal changes in the frame behavior, as is seen in Fig. 5(a). Noticeable changes in the slopes of the hysteretic curves with time can also be observed, as shown in Fig. 5(a). On the third stage of the test, the areas within the curves substantially increase, indicating increase in the absorption of seismic waves [Fig. 5(a)]. The obtained stress–strain relations also show the difference in the responses of the frame to the same input signals, applied to the frame on the second and fourth stages of the test, with a 2 day delay, which is obviously due to changes in the stiffness of the tested frame, as a result of the applied loading.

The estimated stress–strain relations were used to calculate their slopes, averaged over the three floors of the frame and over the oscillations within each time interval; their values are shown in Fig. 5(b). Changes in the slopes of the stress–strain relations indicate changes in the shear moduli of the frame. According to the estimates, the decrease in the shear moduli was observed during the first ($\sim$50% of the initial values), second ($\sim$15% of the initial values), and fourth ($\sim$15% of the initial values) stages of the test, whereas at the third stage they remained approximately at the same level. As far as these conclusions and the following nonlinear identification of the frame behavior under the dynamic loading are based on the constructed model of the behavior of the frame, it would be useful to validate our conclusions by analyzing records, obtained in the test. An agreement of estimates made for the model with the experimental data would testify to the validity of the model and of our conclusions.

Identification of Impulse Response Function

Based on the proposed method the impulse characteristics of the frame $h_1(\tau)$ was estimated, obtained in the tests (Fig. 6). Each characteristic reflects the behavior of the frame at a certain stage of the test (first, second, third, or fourth). Oscillating character of impulse characteristics $h_1(\tau)$ at the first and second stages of the test (Fig. 6, 1 and 2) indicates multiple reflections of seismic waves in the frame at these stages. At the third stage of the test, amplitudes of oscillations substantially decrease, and absorption increases (Fig. 6, 3), which is in good agreement with the results obtained for the model.

The maxima of $h_1(\tau)$, corresponding to times of propagation of seismic waves from the bottom of the frame to the third floor, shift to larger time delays during the test (Fig. 6), was also examined. The propagation times increased from $\sim$0.14 s at the first stage of the test to $\sim$0.18–0.2 s at the second and third stages and to $\sim$0.24–0.26 s at the fourth stage of the test. This confirms our conclusions, obtained for the model, concerning the decrease of the shear moduli in the frame at the first and fourth stages of the test, if we take into account that in calculating $h_1(\tau)$, the main contribution comes from intervals of higher intensity, i.e., the middle and beginning parts of the records.

Nonlinear Identification

Since stress–strain relations determine the transformations of incident seismic waves into the system response, nonlinearity of stress–strain relations leads to the appearance of nonlinear components in the response, because it causes distortions in the shapes and spectra of propagating seismic waves. If an input signal is the Gaussian white noise, the relation between an input and

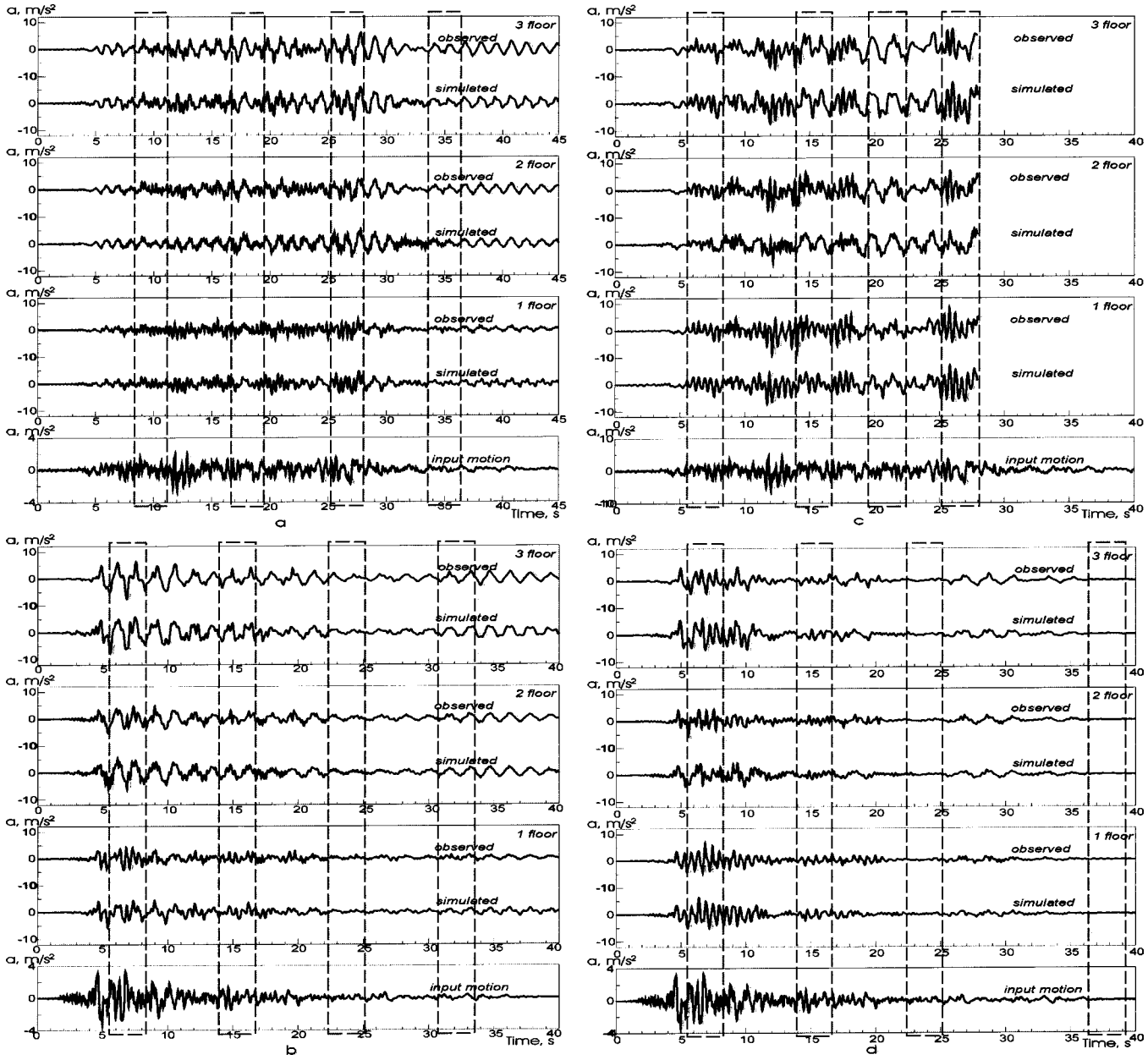

Fig. 4. Simulated and observed acceleration time histories of response of full-scale composite frame recorded at three stories; dashed lines indicate time intervals selected for nonlinear identification of behavior of frame; the imposed ground motion is also shown; (a) for the case of the October 11 test; (b) for the case of the October 14 test; (c) for the case of the October 15 test; and (d) for the case of the October 16 test

an output of a nonlinear system can be represented as the Wiener series (Marmarelis and Marmarelis 1978)

$$y(t)=\sum_{m=0}^{\infty} G_m[h_m(\tau_1,\ldots,\tau_m);x(t'),t'\leqslant t], \tag{3}$$

where $y(t)$=output; G_m=orthogonal functionals if $x(t)$ is the Gaussian white noise with a zero mean; $\{h_m(\tau_1,\ldots,\tau_m)\}$ =sequence of the Wiener kernels; and $\tau_1,\ldots,\tau_m$=time delays. Each kernel is a symmetric function. The first four Wiener functionals are represented in the form

$$G_0[h_0;x(t)]=h_0 \tag{4}$$

$$G_1[h_1;x(t)]=\int_0^{\infty} h_1(\tau)x(t-\tau)d\tau \tag{5}$$

$$G_2[h_2;x(t)]=\int_0\int^{\infty} h_2(\tau_1,\tau_2)x(t-\tau_1)x(t-\tau_2)d\tau_1\,d\tau_2 - P\int_0^{\infty} h_2(\tau_1,\tau_1)d\tau_1 \tag{6}$$

$$G_3[h_3;x(t)]=\int\int_0^{\infty}\int h_3(\tau_1,\tau_2,\tau_3)x(t-\tau_1)x(t-\tau_2) \times x(t-\tau_3)d\tau_1\,d\tau_2\,d\tau_3-3P \times\int_0\int^{\infty} h_3(\tau_1,\tau_2,\tau_2)x(t-\tau_1)d\tau_1\,d\tau_2 \tag{7}$$

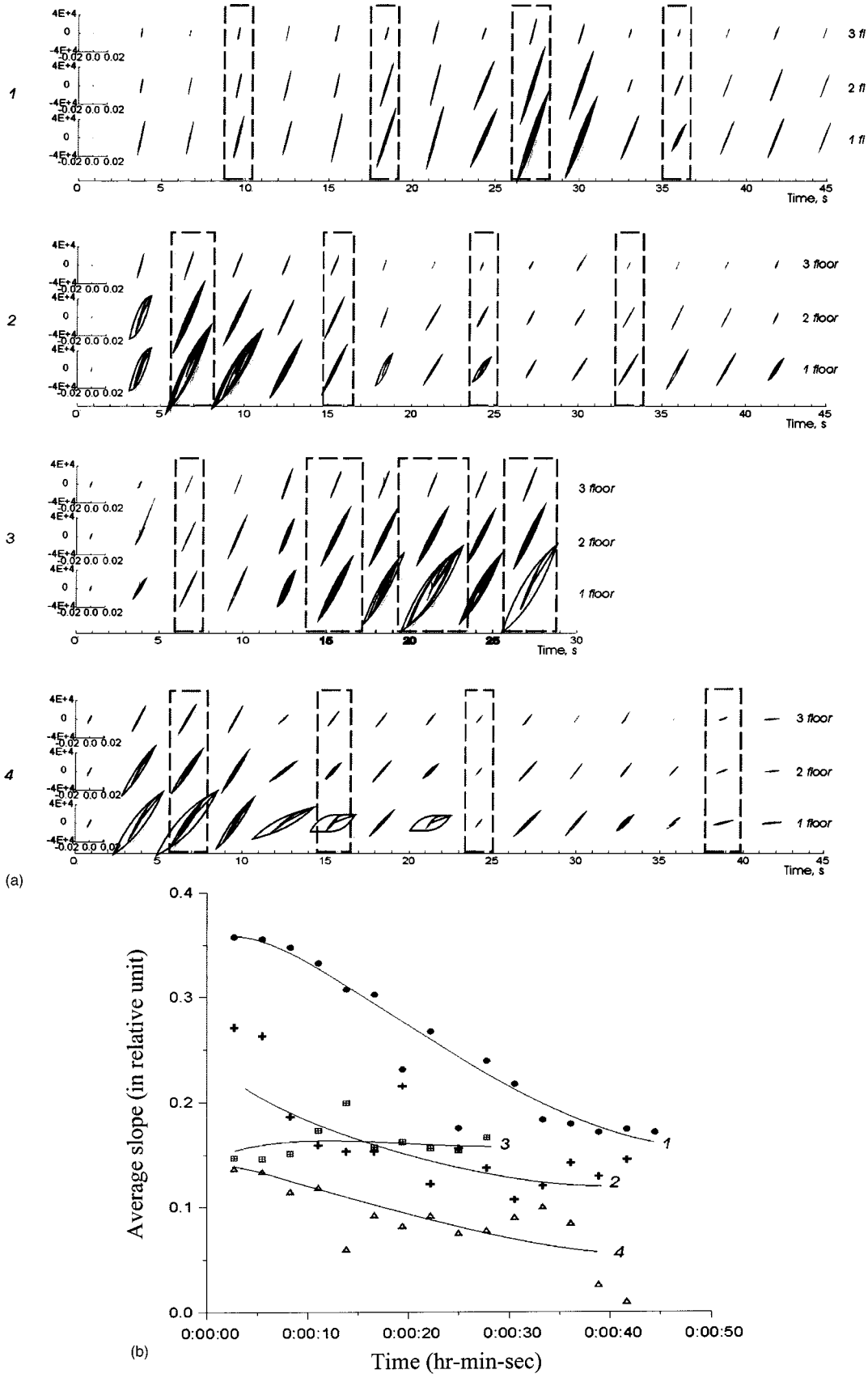

Fig. 5. (a) Obtained stress–strain relations for different time windows from four tests referred to in Fig. 4. Stresses are given in kPa and strains are given in strains. Dashed lines indicate time intervals selected for nonlinear identification of behavior of frame (1, 2, 3, and 4 correspond to four successive stages of test); and (b) decrease in slopes of obtained stress–strain relations with respect to time, reflecting reduction of shear moduli of frame during four tests

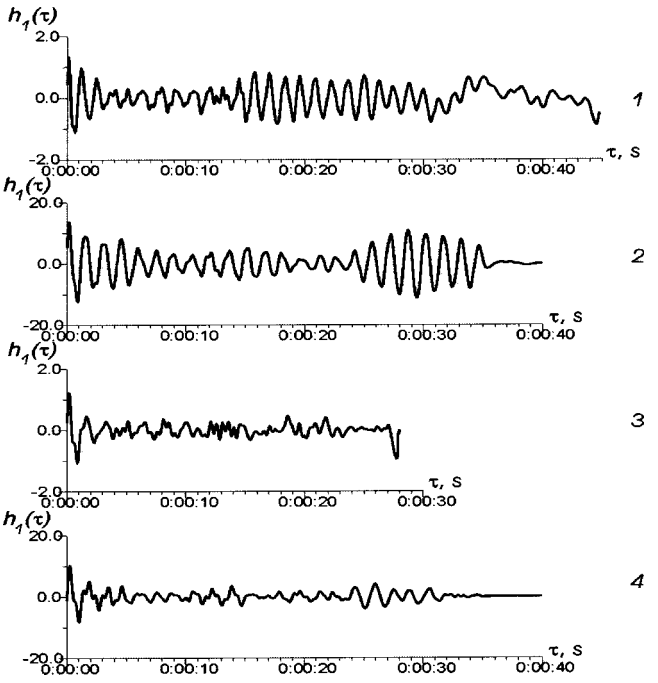

Fig. 6. Identified impulse characteristics based on records obtained from four different tests

where τ=time delay; and P=intensity of the white noise not depending on frequency.

Using the Gaussian white noise as an input signal provides essential advantages in describing nonlinear systems: Orthogonality of terms in the Wiener series with respect to the Gaussian white noise allows application of the effective methods of estimating kernels, based on determination of cross-correlation functions; from the other side, the Gaussian white noise as an input signal allows the most effective testing of the system, because it contains components of all frequencies and amplitudes.

By analogy with an ordinary impulse characteristic $h(t)$, the kernel series $\{h_m\}$ can be treated as a generalized composed impulse characteristic of a system. The first-order kernel determines the linear part of the system response, whereas higher-order kernels describe interactions between the values of the input signal in the past with respect to their influence on the response at present (Marmarelis and Marmarelis 1978). If a system is linear, $h_2(\tau_1,\tau_2)=h_3(\tau_1,\tau_2,\tau_3)=\ldots=0$, and knowledge of the first term of the Wiener series, i.e., knowledge of the first-order kernel $h_1(\tau)$, is sufficient to describe the system. To describe a nonlinear system, several terms of the Wiener series are necessary. Thus, to estimate the contents of the linear and nonlinear components in the response of the frame, we calculated the propagation of the Gaussian white noise in the frame by using previously obtained stress–strain relations. Kernels h_0, $h_1(\tau)$, $h_2(\tau_1,\tau_2)$, and $h_3(\tau_1,\tau_2,\tau_3)$ were estimated by the method of cross-correlation functions, described in Marmarelis and Marmarelis (1978).

Dashed lines in Figs. 4(a–d) and Fig. 5(a) mark time intervals selected for the nonlinear identification of the behavior of the frame. Nonlinear identification allows us to distinguish a linear part of the system response and nonlinear corrections, which are due to various types of nonlinearity, and estimate their contributions to the response of the system; it allows determination of the types and quantitative characteristics of the system nonlinearity (Marmarelis and Marmarelis 1978).

As is seen from formulas (3)–(7), the contents of linear and nonlinear components in the response of a nonlinear system depend on the intensity of the testing signal. Therefore, an adequate choice of the intensity of the testing Gaussian white noise is important for obtaining faithful results. Evidently, we should choose such intensity of the testing Gaussian white noise that the contents of the nonlinear components in the response of a system studied to the Gaussian white noise were similar to that in its response to the dynamic loading applied in the test. Since the nonlinearity of the system response is determined by the nonlinearity of its stress–strain relations, this study chose Gaussian white noise as the testing input signal so that average stresses and strains occurring in the frame during the propagation of the Gaussian white noise, coincide with stresses and strains occurring in the frame under the dynamic loading in the test.

Based on the study of nonlinear acoustics (for example, Zarembo and Krasil'nikov 1966), monochromatic signals, passed through a nonlinear filter, acquire higher harmonics of their main frequencies. To emphasize these phenomena, a Gaussian white noise was selected as an input, and then the nonlinear quadratic, cubic, and higher-order components of the frame response were calculated by estimating the Wiener functionals by the method of cross-correlation functions. The intensities of the quadratic, cubic, and higher-order components of the response can be expressed in percent of the whole intensity of the response.

Nonlinear Identification with Respect to Different Time Windows

Figs. 7, 8, 9, and 10 represent the results of the nonlinear identification of the response of the frame at the four stages of the test, respectively. Four time intervals are analyzed at each stage of the test, which are marked in Figs. 4(a–d) and Fig. 5(a). The Gaussian white noise was used as an input signal, and in each time interval we chose the intensity of the Gaussian white noise so that stresses and strains that occurred in the frame were similar to those that occurred in the frame in conditions of the dynamic loading applied in the test. In the upper parts of Figs. 7–10, the identified first-order impulse characteristics of the model of the frame behavior $h_1(\tau)$ and the diagonal values of its impulse characteristics of the second and third orders $h_2(\tau_1,\tau_2)$ and $h_3(\tau_1,\tau_2,\tau_3)$ are shown. The oscillating character of $h_1(\tau)$ indicates an important role of reflections in the propagation of seismic waves in the frame. A decrease in the amplitudes of oscillations of the first-order impulse characteristics $h_1(\tau)$ is observed, most clearly appearing at the fourth stage of the test. This indicates an increase in the absorption of seismic waves in the frame and agrees well with that observed in the test data. Maxima of the first-order impulse characteristics $h_1(\tau)$ shift to larger time delays, and the periods of oscillations of $h_1(\tau)$ increase, which is due to decrease in the elastic shear moduli of the frame.

Diagonal values of the second- and third-order impulse characteristics $h_2(\tau_1,\tau_2)$ and $h_3(\tau_1,\tau_2,\tau_3)$ are scaled in the same manner for comparison. It is concluded that coefficients at the quadratic terms in expressions describing the respective stress–strain relations, are usually substantially smaller than coefficients at the cubic terms. Multiple reflections of seismic waves in the frame appear in the oscillating shapes of the second- and third-order impulse characteristics $h_2(\tau_1,\tau_2)$, and $h_3(\tau_1,\tau_2,\tau_3)$. The variability of the amplitudes of the diagonal values of the second- and third-order impulse characteristics, which does not show any definite tendency, is due to the fact that these amplitudes depend not only on the shapes of the stress–strain relations, but also on

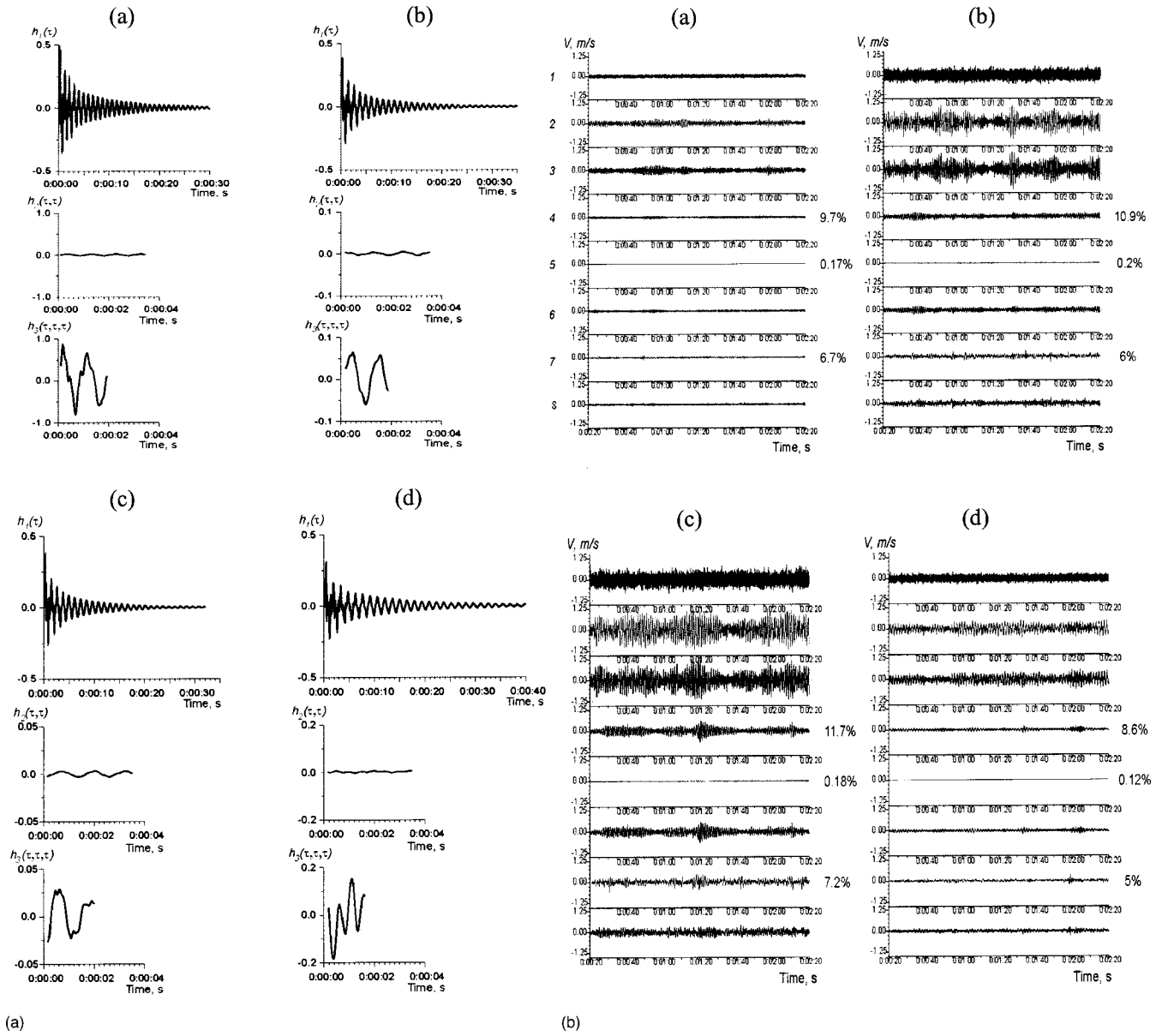

Fig. 7. (a) First-order, second-order, and third-order impulse response functions identified from four different time windows (shown in Fig. 4) of first test data; and (b) Gaussian white noise was used as input to identified system [shown in (a)] and results of nonlinear identification of different time window

the average stresses and strains excited in the frame, which vary during its loading, according to changes in the intensities of input signals.

In Figs. 7–10, the results of the nonlinear identification of the behavior of the frame under the dynamic loading are presented. ''1'' indicates the Gaussian white noise, approximating the imposed motion in the test, which was used as an input signal; ''2'' is the calculated response of the frame to the Gaussian white noise; ''3'' is the response predicted by a linear model; ''4'' is the difference between the response of the frame and the response predicted by the linear model; ''5'' is the nonlinear correction due to quadratic nonlinearity of the frame; ''6'' is the difference between the response of the frame and the response predicted by the linear model with the nonlinear quadratic correction; ''7'' is the nonlinear correction due to cubic nonlinearity of the frame; and ''8'' is the difference between the response of the frame and the response predicted by the linear model with the nonlinear quadratic and cubic corrections. Discussions are made based on these nonlinear identifications.

1. The contents of linear and nonlinear components in the frame response are estimated in percent of the intensities of the response (Figs. 7–10). Table 1 shows estimates of the nonlinear components averaged over the stages of the test. The last two columns represent the ratios of the nonlinear quadratic and cubic components and the residual parts of the frame response, which are the differences between the responses of the frame and the responses predicted by linear models with the nonlinear quadratic and cubic components (rows 8 in Figs. 7–10).
2. As is seen from Table 1, the whole nonlinear component and the nonlinear quadratic and cubic components of the frame response increase in successive loadings of the frame tested.

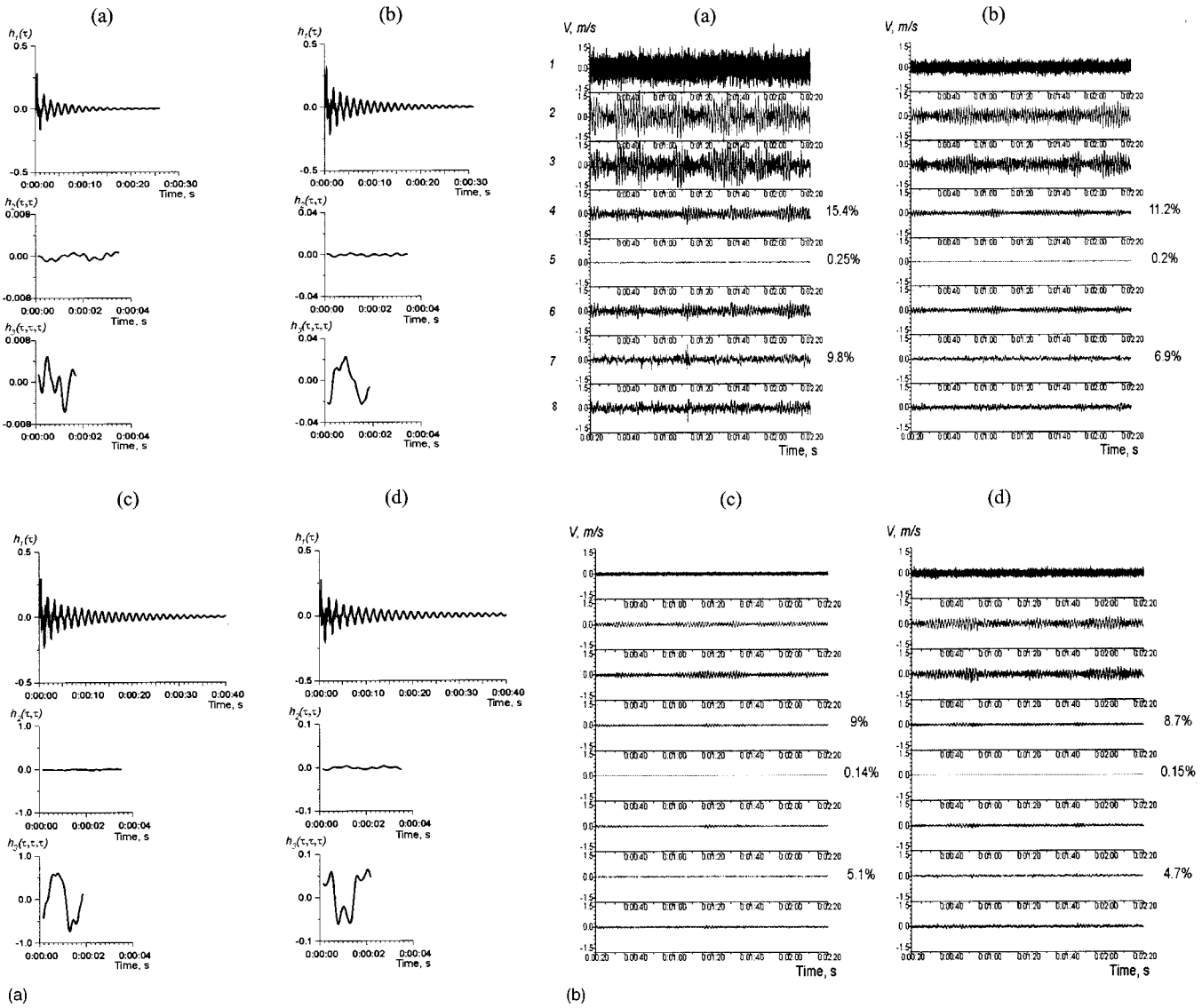

Fig. 8. (a) First-order, second-order, and third-order impulse response functions identified from four different time windows (shown in Fig. 4) of second test data; and (b) Gaussian white noise was used as input to identified system [shown in (a)] and results of nonlinear identification of different time window

The residual part of the frame response is due to the nonlinear components of higher orders, such as, the fourth, fifth, sixth, etc., as well as to inaccuracies in the estimates. This part of the response also shows the tendency of increasing with time. Zero-order components of the responses h_0 are very small, and their values are not given.

3. Intensities of the nonlinear cubic components of the response are substantially higher than that for the nonlinear quadratic components (Figs. 7–10 and Table 1). This means that the tested frame possesses strong cubic and weak quadratic nonlinearity. Nonlinear systems defined by hysteretic stress–strain relations, similar to those shown in Fig. 5(a), possess not only cubic nonlinearity, but also, other odd-order nonlinearities, such as, the fifth, seventh, ninth, eleventh, etc. order nonlinearities, whereas, the role of even-order nonlinearities is usually small (Pavlenko 2001). Therefore, it is concluded that the tested frame possesses mostly odd-order nonlinearities, such as the third, fifth, seventh, ninth, etc. order nonlinearities.
4. However, an increase in the nonlinear quadratic component of the response of the frame during its loading is observed (Figs. 7–10 and Table 1), which is obviously due to changes in the shapes of the stress–strain relations: the stress–strain relations gradually become more sloping and stiffness degradation is observed. This process resembles liquefaction in soils, where similar phenomena are observed (Pavlenko and Irikura 2002). Increase in the nonlinear components in the frame response is obviously related to the decrease in the elastic moduli and strength of the frame tested during its loadings. In this process, stress–strain relations change their shapes and slopes, and the domain of the linear elastic behavior of the frame decreases and shifts to smaller strains. In this case, the nonlinear components of the response obviously increase.
5. Inaccuracies in the estimates are analyzed, and correction methods are given in the paper by Marmarelis and Marmarelis (1978). The main causes of the inaccuracies are: The finite duration and the boundedness of the spectral band of the

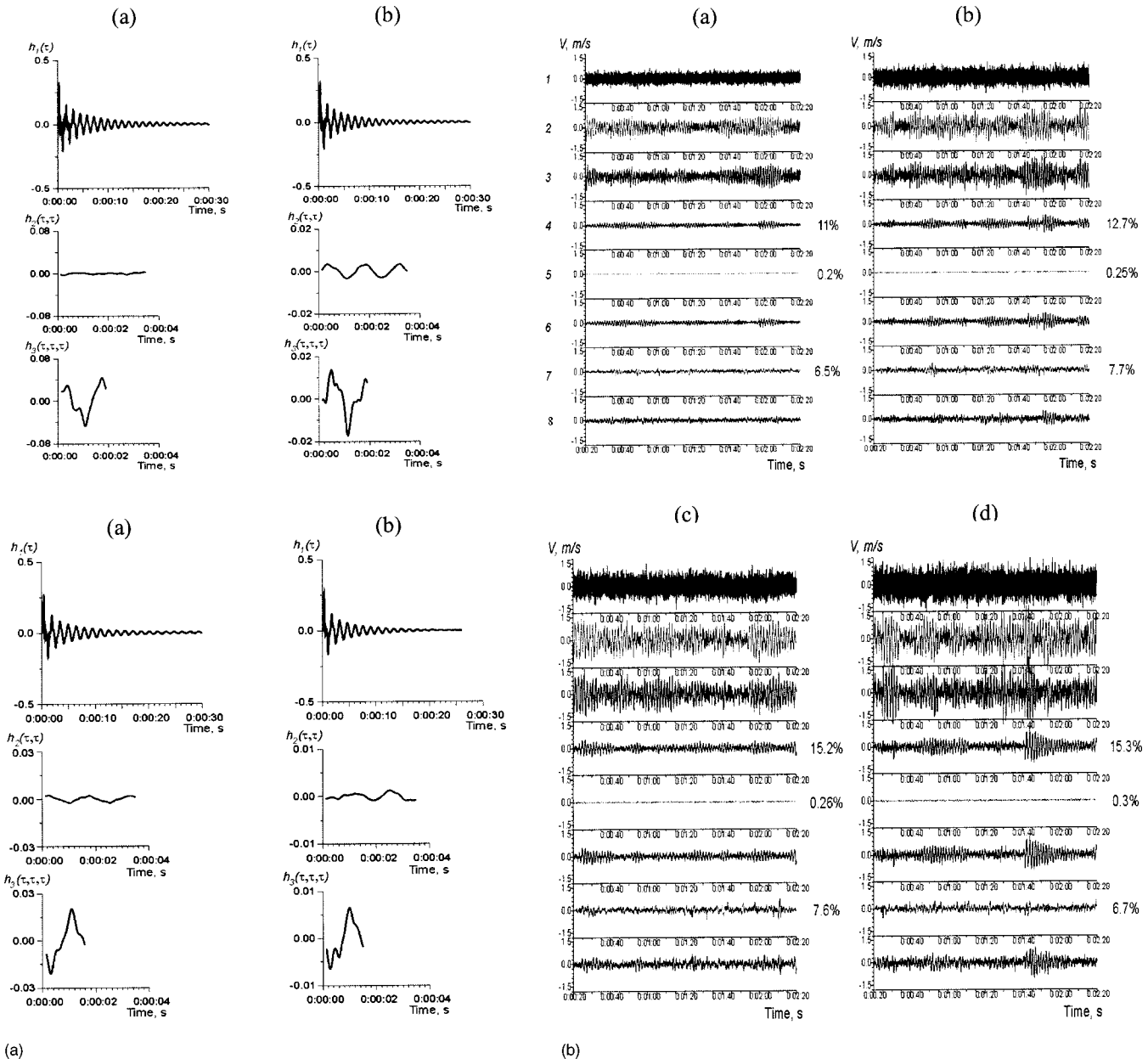

Fig. 9. (a) First-order, second-order, and third-order impulse response functions identified from four different time windows (shown in Fig. 4) of third test data; and (b) Gaussian white noise was used as input to identified system [shown in (a)] and results of nonlinear identification of different time window

Gaussian noise, truncation of tails of normal distribution of noise amplitudes, and inaccuracies in calculations of impulse characteristics, increasing with increase in the order of the characteristic (Marmarelis and Marmarelis 1978). Additional factors causing inaccuracies are evident, such as deviations in the constructed model of the frame behavior from the real behavior of the frame, following inaccurate estimation of stress–strain relations and their working intervals; discrepancies in the contents of nonlinear components in the response of the frame in the test and in the response of its model tested by the Gaussian white noise; and inaccuracies in the profiling data. However, an accurate estimation of the linear and the whole nonlinear component is most important, because further analysis is based on these estimates. Preliminary calculations show us that the accuracy of the estimates in the nonlinear identification in this case can be rather high, and calculation errors usually do not exceed 1–2%, if we use testing Gaussian white noise of a long duration, such as, about 500,000 points, or 3 h. Multiple reflections increase errors in the estimates of linear and nonlinear components up to 3–4%, because in this case, exact knowledge of damping is very important, however, corrections should be similar for all the stages of the test, and they could not influence the tendency of increasing the nonlinear components in the response of the frame.

Conclusions

In this study it is concluded that the method of estimation of nonlinear stress–strain relations, which was previously developed for soils, can be applied for studying the response of engineering

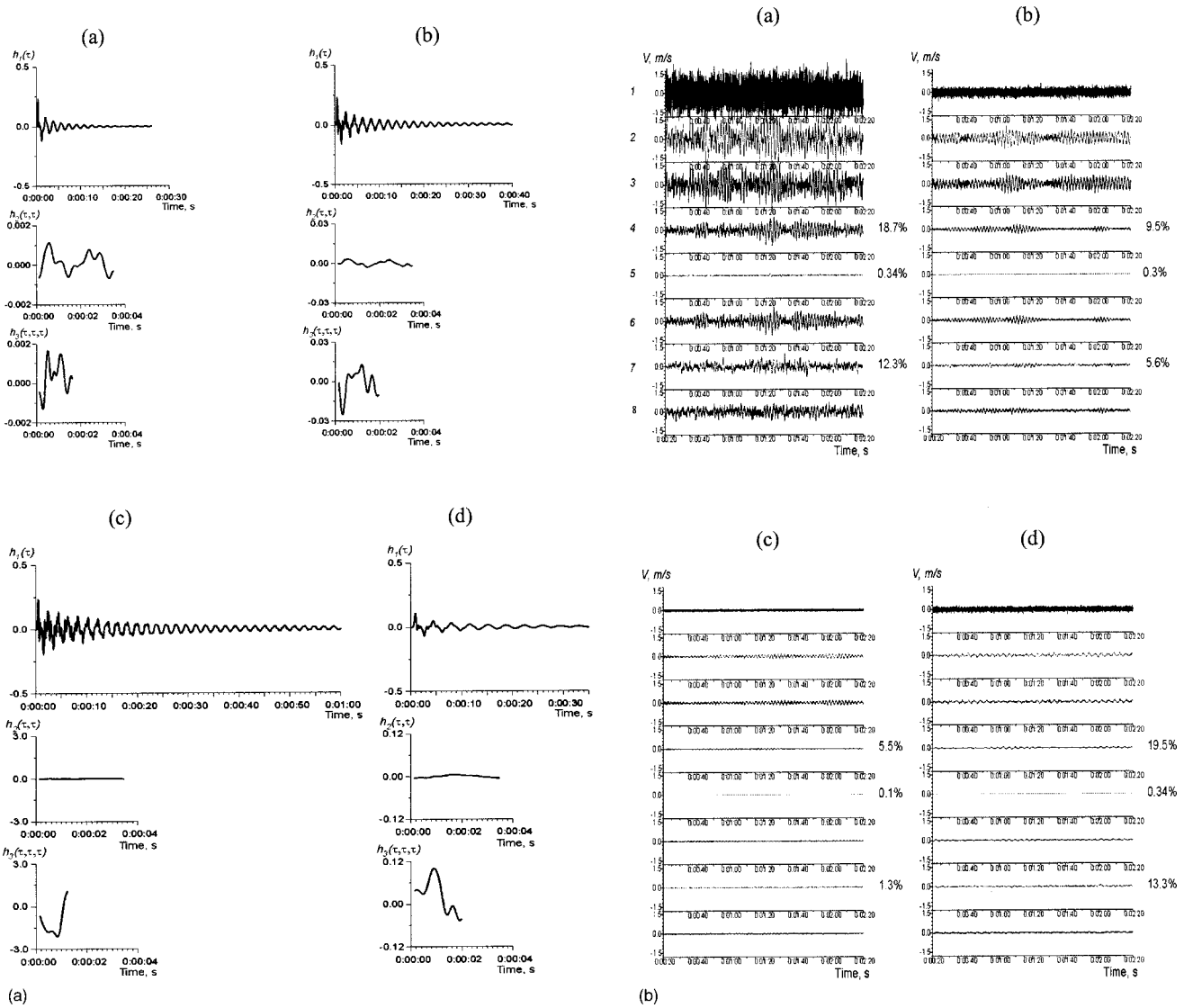

Fig. 10. (a) First-order, second-order, and third-order impulse response functions identified from four different time windows (shown in Fig. 4) of fourth test data; and (b) Gaussian white noise was used as input to identified system [shown in (a)] and results of nonlinear identification of different time window

structures subjected to strong ground motion excitation. Application of this method allows us to obtain information about the behavior of the construction studied and its elastic moduli in successive time intervals. Estimated stress–strain relations can be used for the nonlinear identification of the response of the construction studied in strong ground motion, and a rather accurate estimate of the contents of linear and nonlinear components in the response can be obtained in the case of a proper choice of parameters of testing signals.

Estimated nonlinear stress–strain relations in the three-story full-scale composite moment frame loaded by scaled motions of the 1999 Chi-Chi Earthquake and the 1989 Loma Prieta Earthquake in the joint tests of the National Center for Research in Earthquake Engineering in Taipei and Stanford Univ. show a substantial decrease in the elastic shear moduli in the frame by ~70% of their initial values during the tests. At the same time, absorption of seismic waves in the frame increased, and the contents of nonlinear components in the frame response increased from about 8.5–11% to about 15.5–19.5%, which was due to the increase of odd- and even-order components in the response. It was found that the frame possesses mostly odd-order nonlinearities, such as the third, fifth, seventh, ninth, etc. order nonlinearities, whereas, the even-order nonlinearities are weak. However, part of the even-order nonlinearities increased during the tests, which is due to changes in shapes of the stress–strain relations. Similar phenomena are observed in liquefaction of soils.

Table 1. Estimates of Contents of Nonlinear Components of Frame Response Averaged over Stages of Test

Stage of the test	Whole nonlinear component (%)	Nonlinear quadratic component (%)	Nonlinear cubic component (%)	Ratio of nonlinear quadratic to nonlinear cubic components	Residual (%)
1	10.2	0.17	6.2	0.027	8.7
2	11.1	0.25	6.6	0.029	8.9
3	13.6	0.32	7.1	0.036	11.9
4	13.3	0.27	8.1	0.046	10.6

Acknowledgments

This research was supported by the National Science Council (Taiwan) under Grant No. NSC91-2211-E-002-079. Pseudodynamic test data of the RCS frame provided by Professor K. C. Tsai (NCREE) are greatly appreciated.

Notation

The following symbols are used in this paper:

$G_m[\cdot]$ = orthogonal functions;
$h_1(\tau_1)$ = first-order impulse response function;
$h_2(\tau_1,\tau_2)$ = second-order impulse response function;
$h_3(\tau_1,\tau_2,\tau_3)$ = third-order impulse response function;
P = intensity of white noise;
$\ddot{u}_i(t)$ = recorded acceleration at level z_i;
γ_i = shear strain at level z_i;
ρ_i = mass density; and
τ_i = shear stress at level z_i.

References

Hunter, N. F. (1990). ''Analysis of nonlinear systems using ARMA models.'' *Proc., 8th Int. Modal Analysis Conf.*, 341–347.

Joyner, W. B., and Chen, T. F. (1975). ''Calculation of nonlinear ground response in earthquakes.'' *Bull. Seismol. Soc. Am.*, 65, 1315–1336.

Korenberg, M., Billings, S. A., Liu, Y. P., and McIlroy, P. J. (1987). ''Orthogonal parameter estimation algorithm for nonlinear stochastic systems.'' *Int. J. Control*, 48, 193–210.

Loh, C. H., and Duh, J. Y. (1996). ''Analysis of nonlinear system using NARMA model.'' *J. Struct. Eng./Earthquake Eng.*, 537, I-35.

Loh, C. H., Wu, T. Z., Tseng, C. C., and Kao, C. Y. (2003). ''Experimental study of identification of RCS structure: Using pseudo-dynamic test data.'' *Proc., Int. Conf. on Structural Health Monitoring and Intelligent Infrastructure*, Z. Wu and M. Abe, eds., Vol. 1, A. A. Balkema, Tokyo, 437–445.

Marmarelis, P. Z., and Marmarelis, V. Z. (1978). *Analysis of physiological systems, the white-noise approach*, Plenum, New York.

Pavlenko, O. V. (2001). ''Nonlinear seismic effects in soils: Numerical simulation and study.'' *Bull. Seismol. Soc. Am.*, 91, 381–396.

Pavlenko, O. V., and Irikura, K. (2002). ''Changes in shear moduli of liquefied and nonliquefied soils during the 1995 Kobe earthquake and its aftershocks at PI, SGK, and TKS vertical array sites.'' *Bull. Seismol. Soc. Am.*, 92(5), 1952–1969.

Pavlenko, O. V., and Irikura, K. (2003). ''Estimation of nonlinear time-dependent soil behavior in strong ground motion based on vertical array data.'' *Pure Appl. Geophys.*, in press.

Schetzen, M. (1980). *The Voltera and Weiner series of nonlinear systems*, Wiley, New York.

Zarembo, L. K., and Krasil'nikov, V. A. (1966). *Introduction to nonlinear acoustics*, Nauka, Moscow.